## Title

A pivotal role of androgen signaling in Notch-responsive cells in prostate development, maturation, and regeneration



## Authors

Aldahl, Joseph
Yu, Eun-Jeong
He, Yongfeng
et al.

## Publication Date

2019-05-01

## DOI

10.1016/j.diff.2019.03.002

Peer reviewed

HHS Public Access

Author manuscript

*Differentiation*. Author manuscript; available in PMC 2020 May 01.

Published in final edited form as:

*Differentiation*. 2019 ; 107: 1–10. doi:10.1016/j.diff.2019.03.002.

# A Pivotal Role of Androgen Signaling in Notch-Responsive Cells in Prostate Development, Maturation, and Regeneration

**Joseph Aldahl**[1,¶], **Eun-Jeong Yu**[1,2,¶], **Yongfeng He**[1,2], **Erika Hooker**[1,2], **Monica Wong**[1], **Vien Le**[1], **Adam Olson**[1], **Dong-Hoon Lee**[1], **Won Kyung Kim**[1], **Charles L. Murtaugh**[3], **Gerald R. Cunha**[4], and **Zijie Sun**[1,2]

[1]Department of Cancer Biology, Beckman Research Institute, City of Hope, Duarte, CA 91010;

[2]Department of Urology, Stanford University School of Medicine, Stanford, CA 94305-5328;

[3]Department of Human Genetics, University of Utah, Salt Lake City, UT 84112,

[4]Department of Urology, School of Medicine, University of California San Francisco, San Francisco, CA 94143

## Abstract

Androgen signaling is essential for prostate development, morphogenesis, and regeneration. Emerging evidence also indicates a regulatory role of Notch signaling in prostate development, differentiation, and growth. However, the collaborative regulatory mechanisms of androgen and Notch signaling during prostate development, growth, and regeneration are largely unknown. Hairy and Enhancer of Split 1 (Hes1) is a transcriptional regulator of Notch signaling pathways, and its expression is responsive to Notch signaling. Hes1-expressing cells have been shown to possess the regenerative capability to repopulate a variety of adult tissues. In this study, we developed new mouse models to directly assess the role of the androgen receptor in prostatic Hes1-expressing cells. Selective deletion of AR expression in embryonic Hes1-expressing cells impeded early prostate development both *in vivo* and in tissue xenograft experiments. Prepubescent deletion of AR expression in Hes1-expressing cells resulted in prostate glands containing abnormalities in cell morphology and gland architecture. A population of castration-resistant Hes1-expressing cells was revealed in the adult prostate, with the ability to repopulate prostate epithelium following androgen supplementation. Deletion of AR in Hes1-expressing cells diminishes their regenerative ability. These lines of evidence demonstrate a critical role for the AR in Notch-responsive cells during the course of prostate development, morphogenesis, and regeneration, and implicate a mechanism underlying interaction between the androgen and Notch signaling pathways in the mouse prostate.

**Correspondence:** Zijie Sun, Ph.D., MD, Beckman Research Institute and Cancer Center, Beckman Bldg., Room 2311, 1500 Duarte Road, Duarte, CA 91010-0300, Tel: (626) 218-0955, zjsun@coh.org.
¶These two authors contributed equally to the work.



The authors declare no potential conflicts of interest.

**Keywords**

Prostate; Androgen receptor; Notch; Hes1; Mouse models; Development

## INTRODUCTION

The prostate gland is a male accessory reproductive organ that contributes a significant portion of the components of seminal fluid during ejaculation (Cunha et al., 1987). In the mouse, prostate formation starts at embryonic day 16.5 (E16.5), when epithelial buds emerge from the urogenital sinus epithelium, UGE, into the surrounding urogenital sinus mesenchyme, UGM (Prins and Putz, 2008). This biological event is initiated by the activation of the androgen signaling pathways primarily through the androgen receptor (AR) and its ligands, testosterone and 5α-dihydrotestosterone, DHT (Zhou et al., 1994, Cunha et al., 1987). The androgen receptor, AR, is initially expressed in the UGM, and its expression subsequently extends to the UGE (Mirosevich et al., 2005). Androgen signaling remains essential in the regulation of prostatic branching and ductal patterning between postnatal days 15 and 30 (P15–30), morphogenesis and growth during puberty (P25–40), and maturation and regeneration in adulthood (Brennen and Isaacs, 2018).

The Notch signaling pathway is a potent regulator of embryonic development, cell lineage commitment, and tissue growth and regeneration (Sato et al., 2012, Deng et al., 2016, Orr et al., 2009). Notch signaling is initiated by the interaction between a Notch ligand membrane protein and a Notch receptor on an adjacent cell (Teoh and Das, 2018). The interaction with the ligand changes Notch receptor conformation and allows for its cleavage by an ADAM (a disintegrin and metalloprotease) followed by a gamma-secretase, releasing the Notch Intracellular Domain (NICD) which moves in to the nucleus and regulates transcriptional activity of target genes, including Hairy and Enhancer of Split 1, Hes1 (Pedrosa et al., 2016). Hes1 is a transcriptional regulator of Notch signaling via a negative feedback mechanism (Deng et al., 2016). Previous studies have demonstrated a positive correlation between Hes1 expression and progenitor cells in hematopoiesis (Kunisato et al., 2003), GI tract maintenance (Kobayashi and Kageyama, 2014), and pancreatic development and homeostasis. Lineage tracing Hes1-expressing cells in the pancreas revealed a dynamic expression pattern with stem cell-like properties initially, then contributing to an increasingly restricted mature cell population during adulthood (Kopinke et al., 2011).

Activation of Notch signaling has been observed during the course of prostate embryonic growth and development, pubertal morphogenesis, and tissue regeneration in adulthood (Carvalho et al., 2014). Expression of Notch receptors has been observed in both prostatic luminal and basal epithelial cells (Wang et al., 2006). Emerging evidence has shown a promotional role for Notch/Hes1 signaling in prostate cancer tumorigenesis, progression and metastasis, where the progenitor capabilities of Hes1-expressing cells in prostate epithelium can promote tumor invasion (Hu et al., 2012, Kwon et al., 2014). A repressive role of Notch/Hes1 in regulating the proliferation of prostate progenitor cells was also observed (Shou et al., 2001). The context-dependent nature of Notch signaling in the prostate has made it an area of ongoing investigation. An increase in Notch signaling is observed at discrete

developmental stages in the prostate including embryonic development, puberty, and under castration conditions (Wang et al., 2004). Interestingly, this expression pattern mirrors that of androgen signaling, implying a co-regulation between these two pathways in the prostate (Prins and Putz, 2008). Therefore, characterizing the role of AR in prostatic Notch-responsive cells should provide significant insight into molecular mechanisms underlying androgen and Notch signaling in regulating prostate development and regeneration.

In this study, we employed lineage tracing tools to characterize the expression and cellular identity of Notch-responsive Hes1-expressing cells during prostate early development, postnatal morphogenesis, and regeneration. To assess the specific role of the AR in prostatic Hes1-expressing epithelial cells, we generated $R26^{mTmG/+}$:$Ar^{L/Y}$:$Hes1^{CreERT2/+}$ mice, in which conditional deletion of the *Ar* gene is mediated by inducible Cre activity driven by the Hes1 promoter. Loss of AR in Hes1-expressing cells showed impaired prostate early development, reduced postnatal growth, increased atrophy and epithelial disorganization in the mature gland, and reduced regenerative ability. Together, these results illustrate a regulatory role of Hes1-expressing cells, and indicate their importance in AR-regulated prostate proliferation and differentiation.

## MATERIALS AND METHODS

### Mouse models and mating.

All animal procedures were carried out in accordance with guidelines approved by the Institutional Animal Care and Use Committee at Beckman Research Institute and City of Hope. $Hes1^{CreERT2}$ mice were kindly provided by Dr. Charles Murtaugh (Kopinke et al., 2011). $Ar^{Loxed/Y}$ ($Ar^{L/Y}$) mice were obtained from Dr. Guido Verhoeven (Verhoeven, 2005). $ROSA26^{mTmG/+}$ ($R26^{mTmG/+}$) mice were purchased from Jackson laboratories (stock 7676). Mouse mating was performed following our strategies described previously (He et al., 2018a). Mouse chromosomal DNA samples were isolated for genotyping using genomic PCR approaches with the following primers: Hes1CreER-F: 5'-GGTCCTTACCGGTCATCTGC-3'; Hes1CreER-WT-R : 5'CTCTTAGCCTGCTGCATGTG-3'; Hes1CreER-Mut-R: 5'-CAGCTTGATGAAGATCTGAGC-3'; mTmG-F:5'-CTTCCCTCGTGATCTGCAAC-3'; mTmG WT-R: 5'CAGGACAACGCCCACACA-3'; mTmG Mut-R:5'-GTTATGTAACGCGGAACTCCA-3'; Ar-F: 5'-AGCCTGTATACTCAGTTGGGG-3'; Ar-R: 5'-AATGCATCACATTAAGTTGATACC-3'. Genomic PCR assays were conducted as follows: 94°C for 5 min, followed by 35x (94°C −0:45; 58°C-0:40; 72°C-1:00); 72°C-2:00.

### Mouse procedures.

Tamoxifen (TM) (Sigma-Aldrich) was administered via intraperitoneal (IP) injection. Pregnant females received a single injection 1mg TM per 25g body weight (BW) at either E13.5 or E15.5 for embryonic AR-deletion studies, or 0.5 mg total TM for lineage tracing experiments. Prepubescent male mice received three doses of 1mg TM between postnatal days 14–16 (P14-P16). Adult male mice were given a single dose of 200 μg TM per gram of BW at P56. Castration of adult male mice was performed as described previously (Sugimura et al., 1986). Briefly, both testes and epididymis were removed from anesthetized mice

through a scrotal approach. Upon exteriorization of the testes and epididymis through the scrotal tunica, the distal end of the spermatic cord was ligated with suture. For androgen supplementation experiments, a single testosterone pellet (12.5 mg, Innovative Research of America) was inserted into adult male mice subcutaneously between the scapulae. For kidney capsule implantation, the embryonic urogenital sinus (UGS) was isolated from mouse embryos in pregnant females that received 1mg TM per 25g body weight at E13.5. The UGS was then cultured overnight in DMEM containing 5% FBS, 5% Nu-SerumIV (Corning), 25 μg/mL insulin (Gibco), 10 nM DHT (Sigma), and 1X Penicillin/Streptomycin. The kidney capsule transplantation was performed in 8 week old male SCID as described previously (He et al., 2018a, Lee et al., 2015).

### Histology and Immunostaining.

Mouse tissues were fixed in 10% neutral-buffered formalin and processed into paraffin (Leica Biosystems). Four-micron serial sections were cut and processed from xylene to PBS through a decreasing alcohol gradient. For histological analysis, hematoxylin-eosin staining was performed as described previously (He et al., 2018b, Mi et al., 2018). For immunohistochemistry, slides were boiled in 0.01M citrate buffer (pH 6.0) for antigen retrieval, then peroxidase-depleted by incubation in 0.3% $H_2O_2$ for 15 minutes. Nonspecific antibody binding was blocked with 5% normal goat serum for 30 minutes, followed by incubation in primary antibodies diluted in 1% goat serum at 4°C overnight. Slides were incubated with biotinylated secondary antibodies for 1 hour at room temperature, followed by horseradish peroxidase streptavidin (SA-5004, Vector Laboratories, Burlingame, CA) for 30 min, and stained per manufacturers protocol using DAB substrate (SK-4100, Vector Laboratories). Slides were counterstained with 5% w/v Harris Hematoxylin and mounted with Permount Mounting Medium (SP15–500, Fisher Scientific, Hampton, NH).

For immunofluorescent staining and detection of membrane-bound Tomato (mT) and membrane-bound green fluorescent protein (mGFP) signals, tissues were fixed in 10% neutral-buffered formalin at 4°C overnight, cryoprotected in 30% sucrose at 4°C overnight, and embedded in OCT (Tissue-Tek). Five-micron sections were cut using a Leica cryostat, and slides were washed three times with PBS. For mTmG detection, slides were directly mounted using VECTASHIELD Mounting Medium with DAPI (Vector Laboratories). For immunofluorescence staining, antigen retrieval was performed as described above. Samples were then blocked and incubated overnight with primary antibodies as described above, and washed in PBS, incubated with fluorescent-conjugated secondary antibodies at room temperature for 1 hour, and then mounted as described above.

### Antibodies.

The following primary antibodies were used: anti-GFP (Rabbit, 1:250, 2956, Cell Signaling), anti-GFP (mouse, 1:250, 2955, Cell Signaling), anti-GFP (Chicken, 1:2000, ab13970, Abcam), anti-K5 (rabbit, 1:2400, Biolegend), anti-K8 (mouse, 1:2000, MMS-162P, Biolegend), anti-p63 (rabbit, 1:2000, Biolegend), anti-PCNA (mouse, 1:200, sc-15, Santa Cruz), anti-E-cadherin (mouse, 1:300, c20820, BD Transduction Laboratories), anti-androgen receptor (rabbit, 1:500, PA-15780, Thermo Fisher), Biotinylated anti-rabbit or anti-mouse secondary antibodies (BA-1000 or BA-9200, Vector Laboratories) were used for

immunohistochemistry experiments. For immunofluorescence studies, AlexaFluor-conjugated anti-rabbit, anti-mouse or anti-chicken antibodies were used (Cell Signaling).

### Microscope Image Acquisition.

Images of H&E and immunohistochemistry were acquired on an AxioLab A1 microscope using 10x, 20x, and 40x Zeiss A-Plan objectives with a Canon EOS 1000D camera and using Axiovision software (Carl Zeiss, Germany, http://www.zeiss.com). Images of immunofluorescence staining and mTmG signals were acquired on an Olympus IX81 Inverted Fluorescence Microscope using 10x, 20x, and 40x OlympusPlan Fluor objectives with an QImaging RETIGA 2000R camera and Image-Pro 6.3 software (Media Cybernetics). Cell numbers were counted manually using 40x photomicrographs and ImageJ software. Prostate budding was quantified as previously described (Podlasek et al., 1999). Statistical analyses were performed using 2-tailed Student's *t* test or 2-way ANOVA.

## RESULTS

### Expansion of Hes1-expressing cells co-localizes with AR in embryonic urogenital epithelium

Previous work has identified Notch signaling and Hes1 expression in mouse embryonic urogenital epithelium, UGE (Grishina et al., 2005). In order to assess Hes1 expression during early stages of prostate development, we intercrossed $Rosa26^{mTmG/+}$ and $Hes1^{CreERT2/+}$ mice to generate $R26^{mTmG/+}$:$Hes1^{CreERT2/+}$ mice (Fig. 1A). In these mice, tamoxifen-induced Cre activity results in a permanent genetic mark in the form of a switch from membrane-bound tdTomato (mT) to membrane-bound green fluorescent protein (mG) expression through recombination of the floxed reporter loci in Hes1-expressing cells (Kopinke et al., 2011). The recombined cells can pass the genetic marker, mGFP expression, onto their offspring, thereby allowing the developmental fate of the Notch responsive Hes1-expressing cells to be traced. To assess the expression of Hes1-expressing cells at different embryonic stages, we administered TM to pregnant females at E13.5 and E15.5 and analyzed embryos at E18.5 (Fig. 1B). Hes1-driven GFP positive cells were observed in UGS tissues from embryos administered TM at both E13.5 and E15.5 (Fig. 1C1–D2). The majority of GFP positive cells from the above samples are localized within the UGE areas (arrows, Fig. 1C2 and 1D2). A significant increase in GFP positive cells was observed in tissues labeled at E15.5 in comparison to E13.5 induction (Fig. 1E), indicating an increased activation of Notch signaling in early development of prostate epithelium. Using immunohistochemical approaches, we further assessed the cellular properties of embryonic Hes1-expressing cells in the UGS. As shown in Figures 1F to 1I, the expression of E-cadherin and AR appeared in Hes1-driven GFP-expressing cells at E18.5. These data demonstrate the existence and epithelial cellular identity of Notch-responsive Hes1-expressing cells in mouse embryonic UGS, and the potential for them to give rise to contribute to prostatic epithelium during embryogenesis.

Androgen signaling plays an essential role in prostate early development. The expression of the AR first occurs at the UGM as early as E13.5, and then extends to the UGE areas (Takeda and Chang, 1991). Using co-immunofluorescence (Co-IF) assays, we detected the

expression of AR in Hes1-expressing cells labeled at E13.5 and E15.5 (Fig. 1G and 1H). To further determine the cellular properties of Hes1 and AR co-expressing cells, we performed triple-IF assays using a series of adjacent tissue sections isolated from $R26^{mTmG/+}$:$Hes1^{CreERT2/+}$ embryos labeled at E15.5. The majority of Hes1-activated GFP expressing and AR-positive cells also were positive for E-cadherin staining (white arrowheads, Fig. 2A4–5). A portion of GFP+ and AR+ cells were also positive for CK8 (Fig. 2B4–5) and CK5 (Fig. 2C4–5). In addition, some epithelial Hes1 and AR expressing cells also showed positive staining for p63 (white arrowheads, Fig. 2D4–5), a prostatic progenitor cellular marker (Signoretti et al., 2000). Of note, we also observed scattered cells within the UGM areas that showed AR and GFP-expression in sections from E13.5 and E15.5 induction (blue arrows, Fig. 2A-C4). Taken together, our results demonstrate the cellular properties of prostatic Notch-responsive Hes1-expressing cells in the UGS and suggest a co-regulation between androgen and Notch signaling in prostate early development.

## Loss of AR expression in Hes1-positive cells impairs embryonic prostate budding and morphogenesis.

A primary role ofsNotch signaling during prostate development and tissue regeneration is the promotion of cell lineage commitment (Shou et al., 2001). Androgen signaling is also essential for prostate development. The above embryonic cell tracing experiments have identified a group of Notch-responsive Hes1-expressing cells residing primarily in the UGE area. The expression of AR also occurs in these Hes1-expressing epithelial cells. To directly assess the role of AR in prostatic Hes1 expressing cells, we developed a new mouse model, $R26^{mTmG/+}$:$Ar^{L/Y}$:$Hes1^{CreERT2/+}$, in which the deletion of the *Ar* gene and expression of GFP are induced specifically in Hes1-expressing cells by tamoxifen (TM) induced recombination (Fig. 3A). TM was administered to pregnant females at 13.5 days post-conception (E13.5) and embryos were isolated and analyzed at E18.5. Hes1-driven GFP expression was primarily revealed in the UGE areas of both $R26^{mTmG/+}$:$Hes1^{CreERT2/+}$ and $R26^{mTmG/+}$:$Ar^{L/Y}$:$Hes1^{CreERT2/+}$ mice (Fig. 3C1–3 and 3D1–3). Normal prostatic budding was apparent in $R26^{mTmG/+}$:$Hes1^{CreERT/+}$ mice (blue arrows, Fig. 3C1–3). Cellular characteristics of the prostatic buds were further assessed by co-IF for E-cadherin and Nkx3.1 expression in the above UGS tissues (Fig. 3C2–3). In contrast to the normal budding seen in control mice, aberrant prostatic budding was observed in the UGS tissues isolated from $R26^{mTmG/+}$:$Ar^{L/Y}$:$Hes1^{CreERT2/+}$ embryos at E18.5 (Fig. 3D1–3). Significant reduction of prostatic budding was observed in the AR-deficient UGS tissues (Fig. 3G right panel), with fewer total buds and epithelial disorganization throughout the UGE (pink arrows, Fig. 3D1–3). Using coimmunofluorescence (Co-IF) assays, we assessed AR expression in the above UGS tissues. While uniform nuclear staining was observed in GFP-positive cells in $R26^{mTmG/+}$:$Hes1^{CreERT2/+}$ embryos, a significant reduction of AR expression was observed in the UGS tissues of $R26^{mTmG/+}$:$Ar^{L/Y}$:$Hes1^{CreERT2/+}$ embryos (Fig. 3E1–1’ versus 3F1–1’, 3G left panel). These data provide a direct link between abnormal budding and AR expression in Hes1-expressing cells during embryogenesis. The epithelial cellular identity of Hes1-expressing cells was also confirmed (Fig. 3E2–2’, and 3F2–2’). Decreased expression of the proliferation marker PCNA was revealed in AR-deficient UGS tissues (Fig. 3F3–3’ versus 3E3–3’). These results provide scientific evidence demonstrating the importance of

AR expression in Notch-responsive Hes1-expressing cells in prostate budding and early development.

To further evaluate the significance and specific role of AR in Hes1-expressing cells during early prostate development, we performed a set of *ex vivo* experiments by implanting UGS tissues isolated from either $R26^{mTmG/+}:Ar^{L/Y}:Hes1^{CreERT2/+}$ or $R26^{mTmG/+}:Hes1^{CreERT2/+}$ male embryos at E15.5 under the kidney capsule of SCID mice (Fig. 4A). Tissues were isolated from the hosts after 8 weeks of implantation, and gross analysis of the xenografts revealed those from $R26^{mTmG/+}:Ar^{L/Y}:Hes1^{CreERT2/+}$ mice were significantly smaller in size and weight compared to those from $R26^{mTmG/+}:Hes1^{CreERT2/+}$ controls (Fig. 4B–C). Histological analyses of AR-deficient grafts displayed abnormalities in gland structure in contrast to normal controls (Fig. 4D1–2'). As shown in the representative images (Fig. 4E1–2'), abnormal prostatic glandular structure appeared with flattened epithelial cells enclosing small acini within a thin, attenuated gland structure. Co-immunofluorescence experiments revealed a significant reduction in AR expression in grafts from $R26^{mTmG/+}:Ar^{L/Y}:Hes1^{CreERT2/+}$ UGS tissues compared to normal controls (Fig. 4F1–1' and 4G1–1'). Co-IF analyses showed that the majority of flattened epithelial cells were positive for CK8 and E-cadherin, but not for CK5, suggesting their derivation from prostatic luminal cells (Fig. 4G2–4'). Together, these results demonstrate a critical role for AR in embryonic Hes1-expressing cells during prostate organogenesis and development.

## Deletion of AR in prepubescent Hes1-expressing cells impairs growth and morphogenesis in the postnatal prostate.

Prostate morphogenesis is completed after birth between postnatal days 15–30 (Prins and Putz, 2008). To examine the effect of AR expression in Hes1-expressing cells during this critical stage of prostate development, $R26^{mTmG/+}:Hes1^{CreERT2/+}$ and $R26^{mTmG/+}:Ar^{L/Y}:Hes1^{CreERT2/+}$ were injected with TM at P14, and analyzed at P56 (Fig. 5A). Histological analysis of $R26^{mTmG/+}:Hes1^{CreERT2/+}$ control mice revealed normal prostatic gland architecture and cellular morphology (Fig. 5B1–2'). In contrast, prostate tissues isolated from AR-deficient mice revealed striking pathological abnormalities resembling the above xenograft tissues, but more severe and penetrant than those observed in implanted embryonic tissues. The prostate tissue from AR-deficient mice at 8 weeks of age showed multiple areas with small abnormal acini within larger glands, frequently enclosed by a thin layer of flattened epithelial cells (blue arrows, Fig. 5C1–C2'), in contrast to normal prostatic glandular context (Fig. 5B1–2'). A significant reduction in AR expression appeared in the prostatic tissues of $R26^{mTmG/+}:Ar^{L/Y}:Hes1^{CreERT2/+}$ mice in comparison with controls (Fig. 5E1 versus 5D1). Specifically, no staining of AR was observed in the abnormal flattened epithelial cells in AR deficient prostate tissues (Fig. 5E1–1'). Co-IF further showed the lack of AR expression in GFP positive cells in the $R26^{mTmG/+}:Ar^{L/Y}:Hes1^{CreERT2/+}$ tissues from mice administered TM at P14 (Fig. 5E3–3'). A decrease in the Proliferating cell nuclear antigen (PCNA)-stained cells was also observed in AR-deficient prostate tissues (Fig. 5E2–2'). These results provide direct evidence of the promotional role for AR in pre-pubertal Notch-responsive cells, as loss of androgen signaling in Notch-responsive cells impairs the maturation and morphogenesis of the postnatal prostate.

### AR expression is required in adult prostatic Hes1-expressing cells for prostate regeneration.

The prostate is an organ with intrinsic regenerative capacity, as the removal of androgen via castration and administration of exogenous testosterone can diminish and regrow the prostate, respectively (Sugimura et al., 1986). To assess the progenitor ability of Notch-responsive Hes1 cells in prostate regeneration, we administered TM to $R26^{mTmG/+}$:$Ar^{L/Y}$:$Hes1^{CreERT2/+}$ mice and their $R26^{mTmG/+}$:$Hes1^{CreERT2/+}$ littermates at 8 weeks of age, and castrated one week later. Four weeks following castration, testosterone was reintroduced in the form of an implanted androgen pellet, potentiating prostate regeneration (Fig. 6A). Prostate tissues were isolated after 4 weeks of regeneration and carefully analyzed. Histological analyses of regenerated prostate tissue from $R26^{mTmG/+}$:$Hes1^{CreERT2/+}$ control mice showed a significant increase in GFP-positive cells in all prostatic lobes compared to castrated tissues (Fig. 6B'-D' versus Fig. 6B–D, 6H left panel). In contrast, fewer, scattered GFP-positive cells appeared in each of the prostatic lobes in regenerated prostates from AR-deficient mice. There was no significant difference in GFP-positive cells between castrated and regenerated conditions in these $R26^{mTmG/+}$:$Ar^{L/Y}$:$Hes1^{CreERT2/+}$ mice (Fig. 6E'–F' versus 6E–F, and 6H right panel). These data demonstrate a requirement of AR expression in Hes1-expressing cells for androgen-induced prostate regeneration.

## Discussion

Formation of the mouse prostate during embryonic development is initiated by the activation of androgen signaling (Sugimura et al. 1986). Mice harboring a mutation resulting in loss of AR function reveal complete absence of prostate tissue, indicating the essential role of the AR in prostate development (Cuhna et al., 1983). While Notch/Hes1 signaling has been implicated in prostatic epithelial budding, branching and differentiation (Grishina et al., 2005), the molecular mechanisms for Notch signaling in androgen-regulated prostate development and growth remain largely unclear. Hes1 is a transcriptional regulator and a downstream target of Notch signaling (Sato et al., 2012). Previous studies have demonstrated the progenitor properties of Notch-responsive Hes1-expressing cells in hematopoiesis as well pancreatic development (Kunisato et al., 2003, Kopinke et al., 2011). In this study, we evaluated the AR expression and activity in Notch-responsive Hes1-expressing cells in prostate development, maturation, and regeneration. We observed the majority of Hes1-expressing cells to be of epithelial origin. Deletion of AR expression in Hes1-expressing cells impairs prostate early development and bud formation, postnatal morphogenesis, and prostate regeneration. Our data provide the first line of evidence to demonstrate an interaction between the androgen and Notch signaling pathways in these critical stages of prostate development.

AR expression has been observed in the UGM as early as E14.5 (Cooke et al., 1991, Shannon and Cunha, 1983, Takeda and Chang, 1991). In our cell tracing experiments, we labeled Hes1-expressing cells at E13.5 and E15.5 and found the majority of Hes1-positive cells occurred within the UGE regions when analyzed at E18.5. An increase in Hes1-positive cells was observed in the samples labeled at E15.5, compared to E13.5. These observations

are consistent with an earlier report that showed a progenitor role of Notch signaling in prostate development (Wang et al., 2004). Of note, while the majority of prostatic Hes1-expressing cells possess epithelial properties, we also observed a smaller population of Hes1-expressing cells scattered through UGM areas (Fig. 2A4–D4). The majority of these cells showed either positive staining for vimentin or smooth muscle actin, suggesting the mesenchymal properties of these cells. This suggests a potential role of Notch signaling in both UGE and UGM during early prostate development. Since prostate budding initiates at E16.5 (Prins and Putz, 2008), we assessed the requirement of AR in Notch-responsive Hes1-positive cells during this developmental stage. We observed decreased and abnormal prostatic budding in UGS tissues of AR-deficient embryos, which provides the first line of evidence demonstrating the biological significance of AR in Hes1-expressing cells. Using UGS tissues isolated from AR-deficient and normal embryonic littermates, we further confirmed the effect of AR in Hes1-expressing cells in prostate development and formation by an *ex vivo* xenograft study. After 8 weeks of xenograft growth, defects were observed in xenograft tissues derived from AR-deleted UGS, including several instances of abnormal, flattened epithelial cells and epithelial atrophy. Our observations illustrate that the AR in embryonic Notch/Hes1-signaling cells is required for normal prostate budding and also plays a key role in regulating the organization and formation of glands during early prostate development.

Similar to the initiation of prostate budding during late embryogenesis, the onset of puberty (P25–40) is a period of rapid growth in prostate size and complexity. The activation of androgen signaling is essential in stimulating pubertal morphogenesis. To assess the importance of AR in Hes1-expressing cells at this stage, we carefully analyzed the prostate tissues in AR-deficient mice, and identified several instances of abnormal, flattened luminal epithelial cells, similar to the implants from AR-deficient embryonic tissues. Moreover, small, abnormal gland-like acini were observed, closed off within areas of normal prostate glands by a thin layer of flattened epithelium. Histological analyses revealed the luminal cell origin of the flattened cells, and the thin monolayer was shown to be fully disconnected from stromal or basal cellular components. The loss of AR expression was also demonstrated in these flattened cells, providing a direct link between AR expression and the aberrant cellular properties. These observations highlight the importance of AR signaling in Notch-responsive cells in postnatal prostate development, and point to a regulatory role for AR in pre-pubertal Notch-responsive cells, as loss of androgen signaling in these cells impairs the maturation and morphogenesis of the postnatal prostate.

It has been shown that prostatic stem/progenitor cells in adult mice are able to survive androgen withdrawal and regenerate upon androgen supplementation (English et al., 1987). In this study, we directly evaluated the regenerative capacity of Notch-responsive cells in the adult prostate, as well as their requirement for AR. We identified a population of Notch-responsive cells that were able to survive in an androgen-depleted environment. Prostates from both $R26^{mTmG/+}$:$Hes1^{CreERT2/+}$ and $R26^{mTmG/+}$:$Ar^{L/Y}$:$Hes1^{CreERT2/+}$ mice showed similar gross and histological responses to castration. Upon reintroduction of testosterone, prostates from $R26^{mTmG/+}$:$Hes1^{CreERT2/+}$ mice were successfully regenerated, and mTmG analysis revealed several clusters of GFP-expressing cells, which demonstrate the regenerative capacity of Notch-responsive Hes1 signaling cells. However, AR-deficient mice

showed a defective ability for regeneration, and no significant increase in GFP-positive cells was observed. These observations demonstrate the important role of Hes1-expressing cells in prostate regeneration, as deletion of AR expression in Notch-responsive Hes1-expressing cells significantly abrogates their regenerative ability.

We have provided multiple lines of evidence to demonstrate that prostatic Hes1-expressing cells possess epithelial cellular properties and play a critical role in androgen signaling-mediated prostate development, postnatal morphogenesis, and regeneration. Our data suggest that Hes1-expressing cells in the prostate are responsive to Notch signaling and regulate prostate development, growth, and regeneration through a co-regulation with androgen-mediated cellular process. The molecular mechanism underlying the interaction between androgen and Notch signaling pathways in prostatic Hes1-expressing cells described here should be further investigated. The advanced mouse genetic tools generated in this study will greatly benefit the future investigations. Further studies on this critical regulation mediated by androgen and Notch signaling pathways will provide fresh insight into our current knowledge on prostate development and growth as well as related prostate tumorigenesis and disorders.

## Supplementary Material

Refer to Web version on PubMed Central for supplementary material.

## Acknowledgements:

This work was supported by NIH grants R01CA070297, R01CA151623, R01CA166894, R21CA190021, and R01DK104941

## Abbreviations:

| | |
|---|---|
| **AR** | androgen receptor |
| **PB** | Probasin |
| **CK** | cytokeratin |
| **UGS** | urogenital sinus |
| **UGE** | urogenital sinus epithelium |
| **UGM** | urogenital sinus mesenchyme |
| **Hes1** | Hairy and Enhancer of Split 1 |
| **DHT** | 5α-dihydrotestosterone |
| **NICD** | Notch Intracellular Domain |
| **R26** | Mouse *Rosa 26* gene locus |
| **TM** | Tamoxifen |
| **mT** | membrane-bound tdTomato (mT) |

| | |
|---|---|
| **mG** | membrane-bound green fluorescent protein (mG) |

## References:


BRENNEN WN & ISAACS JT 2018 The what, when, and why of human prostate cancer xenografts. Prostate, 78, 646–654. [PubMed: 29575112]

CARVALHO FL, SIMONS BW, EBERHART CG & BERMAN DM 2014 Notch signaling in prostate cancer: a moving target. Prostate, 74, 933–45. [PubMed: 24737393]

COOKE PS, YOUNG P & CUNHA GR 1991 Androgen receptor expression in developing male reproductive organs. Endocrinology, 128, 2867–73. [PubMed: 2036966]

CUNHA GR, DONJACOUR AA, COOKE PS, MEE S, BIGSBY RM, HIGGINS SJ & SUGIMURA Y 1987 The endocrinology and developmental biology of the prostate. Endocr Rev, 8, 338–62. [PubMed: 3308446]

DENG G, MA L, MENG Q, JU X, JIANG K, JIANG P & YU Z 2016 Notch signaling in the prostate: critical roles during development and in the hallmarks of prostate cancer biology. J Cancer Res Clin Oncol, 142, 531–47. [PubMed: 25736982]

ENGLISH HF, SANTEN RJ & ISAACS JT 1987 Response of glandular versus basal rat ventral prostatic epithelial cells to androgen withdrawal and replacement. Prostate, 11, 229–42. [PubMed: 3684783]

GRISHINA IB, KIM SY, FERRARA C, MAKARENKOVA HP & WALDEN PD 2005 BMP7 inhibits branching morphogenesis in the prostate gland and interferes with Notch signaling. Dev Biol, 288, 334–47. [PubMed: 16324690]

HE Y, HOOKER E, YU EJ, CUNHA GR, LIAO L, XU J, EARL A, WU H, GONZALGO ML & SUN Z 2018a Androgen signaling is essential for development of prostate cancer initiated from prostatic basal cells. Oncogene.

HE Y, HOOKER E, YU EJ, WU H, CUNHA GR & SUN Z 2018b An Indispensable Role of Androgen Receptor in Wnt Responsive Cells During Prostate Development, Maturation, and Regeneration. Stem Cells, 36, 891–902. [PubMed: 29451339]

HU YY, ZHENG MH, ZHANG R, LIANG YM & HAN H 2012 Notch signaling pathway and cancer metastasis. Adv Exp Med Biol, 727, 186–98. [PubMed: 22399348]

KOBAYASHI T & KAGEYAMA R 2014 Chapter Seven - Expression Dynamics and Functions of Hes Factors in Development and Diseases In: TANEJA R (ed.) Current Topics in Developmental Biology. Academic Press.

KOPINKE D, BRAILSFORD M, SHEA JE, LEAVITT R, SCAIFE CL & MURTAUGH LC 2011 Lineage tracing reveals the dynamic contribution of Hes1+ cells to the developing and adult pancreas. Development, 138, 431–41. [PubMed: 21205788]

KUNISATO A, CHIBA S, NAKAGAMI-YAMAGUCHI E, KUMANO K, SAITO T, MASUDA S, YAMAGUCHI T, OSAWA M, KAGEYAMA R, NAKAUCHI H, NISHIKAWA M & HIRAI H 2003 HES-1 preserves, purified hematopoietic stem cells ex vivo and accumulates side population cells in vivo.

KWON OJ, VALDEZ JM, ZHANG L, ZHANG B, WEI X, SU Q, ITTMANN MM, CREIGHTON CJ & XIN L 2014 Increased Notch signalling inhibits anoikis and stimulates proliferation of prostate luminal epithelial cells. Nat Commun, 5, 4416. [PubMed: 25048699]

LEE SH, JOHNSON DT, LUONG R, YU EJ, CUNHA GR, NUSSE R & SUN Z 2015 Wnt/beta-Catenin-Responsive Cells in Prostatic Development and Regeneration. Stem Cells, 33, 3356–67. [PubMed: 26220362]

MI J, HOOKER E, BALOG S, ZENG H, JOHNSON DT, HE Y, YU EJ, WU H, LE V, LEE DH, ALDAHL J, GONZALGO ML & SUN Z 2018 Activation of hepatocyte growth factor/MET signaling initiates oncogenic transformation and enhances tumor aggressiveness in the murine prostate. J Biol Chem, 293, 20123–20136. [PubMed: 30401749]

MIROSEVICH J, GAO N & MATUSIK RJ 2005 Expression of Foxa transcription factors in the developing and adult murine prostate. Prostate, 62, 339–52. [PubMed: 15389796]

ORR B, GRACE OC, VANPOUCKE G, ASHLEY GR & THOMSON AA 2009 A role for notch signaling in stromal survival and differentiation during prostate development. Endocrinology, 150, 463–72. [PubMed: 18801907]

PEDROSA AR, GRACA JL, CARVALHO S, PELETEIRO MC, DUARTE A & TRINDADE A 2016 Notch signaling dynamics in the adult healthy prostate and in prostatic tumor development. Prostate, 76, 80–96. [PubMed: 26419726]

PODLASEK CA, BARNETT DH, CLEMENS JQ, BAK PM & BUSHMAN W 1999 Prostate Development Requires Sonic Hedgehog Expressed by the Urogenital Sinus Epithelium. Developmental Biology, 209, 28–39. [PubMed: 10208740]

PRINS GS & PUTZ O 2008 Molecular signaling pathways that regulate prostate gland development. Differentiation, 76, 641–59. [PubMed: 18462433]

SATO C, ZHAO G & ILAGAN MX 2012 An overview of notch signaling in adult tissue renewal and maintenance. Curr Alzheimer Res, 9, 227–40. [PubMed: 21605032]

SHANNON JM & CUNHA GR 1983 Autoradiographic localization of androgen binding in the developing mouse prostate. Prostate, 4, 367–73. [PubMed: 6866851]

SHOU J, ROSS S, KOEPPEN H, DE SAUVAGE FJ & GAO WQ 2001 Dynamics of notch expression during murine prostate development and tumorigenesis. Cancer Res, 61, 7291–7. [PubMed: 11585768]

SUGIMURA Y, CUNHA GR & DONJACOUR AA 1986 Morphological and histological study of castration-induced degeneration and androgen-induced regeneration in the mouse prostate. Biol Reprod, 34, 973–83. [PubMed: 3730489]

TAKEDA H & CHANG C 1991 Immunohistochemical and in-situ hybridization analysis of androgen receptor expression during the development of the mouse prostate gland. J Endocrinol, 129, 83–9. [PubMed: 2030333]

TEOH SL & DAS S 2018 Notch Signalling Pathways and Their Importance in the Treatment of Cancers. Curr Drug Targets, 19, 128–143. [PubMed: 28294046]

VERHOEVEN G 2005 A Sertoli cell-specific knock-out of the androgen receptor. Andrologia, 37, 207–8. [PubMed: 16336249]

WANG XD, LEOW CC, ZHA J, TANG Z, MODRUSAN Z, RADTKE F, AGUET M, DE SAUVAGE FJ & GAO WQ 2006 Notch signaling is required for normal prostatic epithelial cell proliferation and differentiation. Dev Biol, 290, 66–80. [PubMed: 16360140]

WANG XD, SHOU J, WONG P, FRENCH DM & GAO WQ 2004 Notch1-expressing cells are indispensable for prostatic branching morphogenesis during development and re-growth following castration and androgen replacement. J Biol Chem, 279, 24733–44. [PubMed: 15028713]

ZHOU ZX, WONG CI, SAR M & WILSON EM 1994 The androgen receptor: an overview. Recent Prog Horm Res, 49, 249–74. [PubMed: 8146426]

## Highlights

In this study, we provide scientific evidence to demonstrate for the first time that selective deletion of AR expression in murine embryonic, prepubescent, or adult Notch-responsive Hes1-expressing cells disrupts prostatic budding, and impairs prostate growth and regeneration. These data demonstrate a critical role of androgen signaling in Notch-responsive cells in regulating prostatic cell fate, growth, and renewal, and further provide scientific evidence for the interaction between androgen and Notch signaling in the prostate.

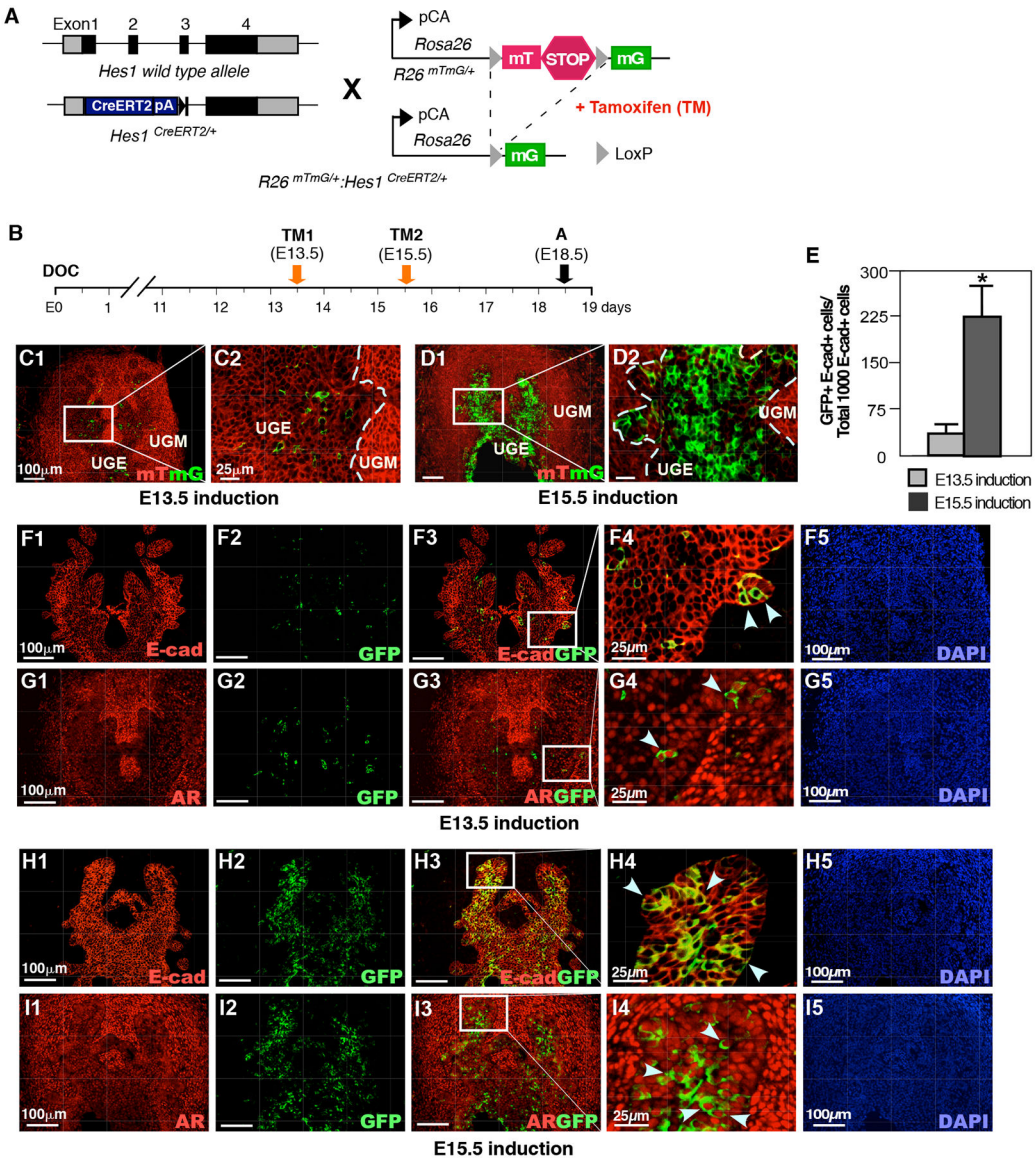


**Figure 1. Hes1 expression in embryonic urogenital development.**

**(A)** Illustration of transgenic alleles in *Rosa26*$^{mTmG/+}$:*Hes1Cre*$^{ERT2/+}$ (*R26*$^{mTmG/+}$:*Hes1Cre*$^{ERT2/+}$) mice. CreERT2: tamoxifeninducible Cre recombinase/estrogen receptor fusion protein, TM: tamoxifen, mG: membrane-bound GFP, mT: membrane-bound tdTomato, pA: polyadenylation-coding region, pCA: chicken beta-actin promoter with cytomegalovirus enhancer. **(B)** Schematic of experimental timeline for TM induction of Cre activity and analysis of urogenital tissues. DOC: day of conception. **(C)** mTmG reporter expression in male urogenital sinus (UGS); TM induction at embryonic day 13.5 (E13.5); analysis at E18.5. UGE: urogenital sinus epithelium, UGM: urogenital sinus mesenchyme. **(D)** mTmG assay on male UGS, TM induction at E15.5; analysis at E18.5. **(E)** Quantification of TM-induced GFP expression at E13.5 or E15.5 in E18.5 urogenital epithelium (UGE). Please also see Supplemental Table 1 in the Supplemental data file. **(F)** Coimmunofluorescent staining (Co-IF) for E-cadherin and GFP in E18.5-male UGS; TM

induction at E13.5, **(G)** Co-IF for androgen receptor (AR) and GFP in E18.5 UGS; TM induction at E13.5. **(H)** Co-IF for E-cadherin and GFP in E18.5-male UGS; TM induction at E15.5. **(I)** Co-IF for AR and GFP in E18.5-male UGS; TM induction at E15.5. Dashed lines delineate UGE and UGM. Arrows indicate GFP+ cells in UGE area. Scale bars: 100 μm, or 25 μm in magnified views. Results are mean +/− SD of at least three independent samples per group. *P<0.05.

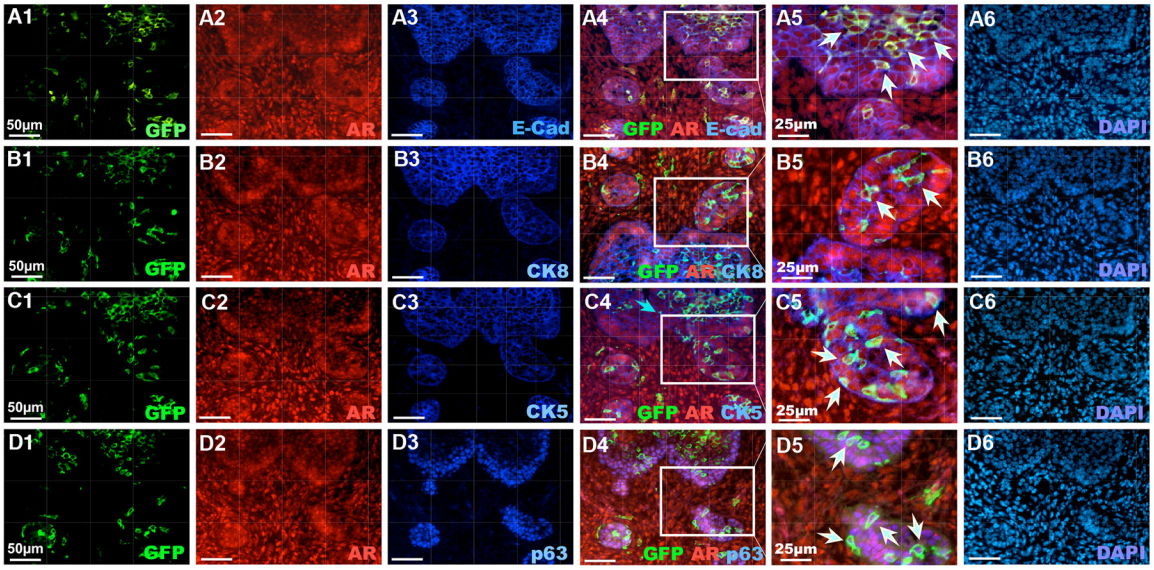


**Figure 2. AR is expressed in Hes1-positive cells during embryonic mouse prostate development.**

Co-IF of the UGS tissues isolated from E18.5 old male *R26*$^{mTmG/+}$*; Hes1Cre*$^{ERT2/+}$ embryos using antibodies as indicated above as well as staining with DAPI. White arrows indicate triple-positive epithelial cells. Scale bars: 50 μm, or 25 μm in A5–D5 sections as labeled above.

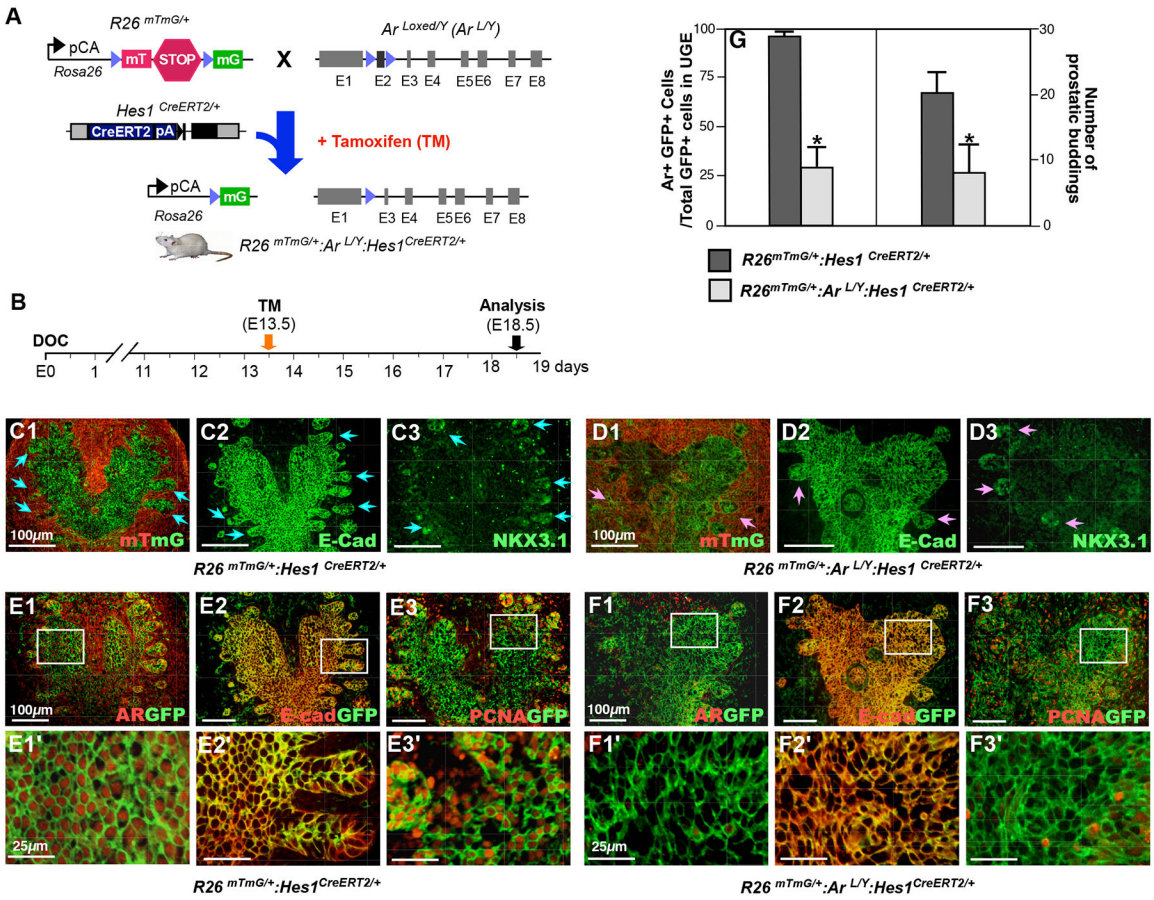


**Figure 3. Deletion of AR expression in Hes1-expressing cells impairs prostate development in vivo.**

**(A)** Illustration of transgenic alleles in *R26*$^{mTmG/+}$*: Ar*$^{L/Y}$*: Hes1Cre*$^{ERT2/+}$ mice. **(B)** Schematic of experimental timeline for tamoxifen induction and analysis of urogenital tissues. **(C1–3)** Analysis of prostatic budding in *R26*$^{mTmG/+}$*: Hes1Cre*$^{ERT2/+}$ mice with mTmG expression (C1), and immunofluorescent (IF) staining with antibodies against E-cadherin (C2), and NKX3.1 (C3). Blue arrows indicate epithelial buddings. **(D1–3)** The similar analyses as described in C1–3 with the UGS tissues of *R26*$^{mTmG/+}$*: Ar*$^{L/Y}$*: Hes1Cre*$^{ERT2/+}$ mice. Pink arrows indicate abnormal epithelial buddings. **(E)** Co-IF analyses of mouse UGS tissues with antibodies as indicated above, GFP and AR (E1), GFP and E-cadherin (E2), or GFP and PCNA (E3) in *R26*$^{mTmG/+}$*: Hes1Cre*$^{ERT2/+}$ E18.5 mouse embryos. **(F)** Similar Co-IF analyses as indicated in E section with tissues from *R26*$^{mTmG/+}$*: Ar*$^{L/Y}$*: Hes1Cre*$^{ERT2/+}$ E18.5 mouse embryos. **(G)** Quantification of AR and GFP co-expressing cells (left panel) and prostatic budding (right panel) in male UGS tissues from indicated genotype embryos. Please also see Supplemental Tables 2 and 3 in the Supplemental data file. Scale bars: 100 μm, or 25 μm in magnified views. Results are mean +/− SD of at least three independent samples from different litters per group. *: P<0.05.

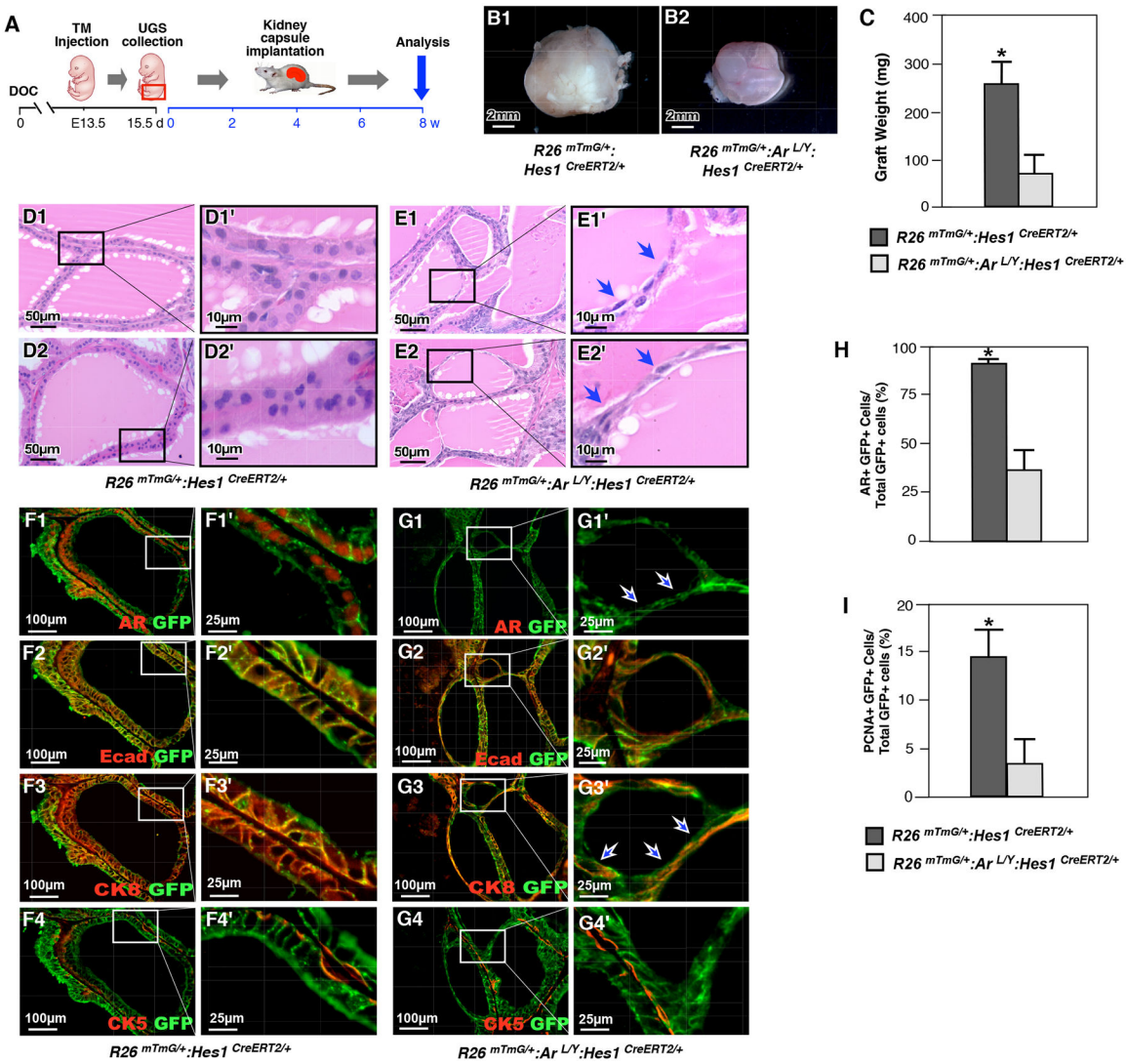


**Figure 4. Deletion of AR in Hes1-expressing cells during embryonic development impedes prostate formation.**

**(A)** Schematic of experimental timeline for TM induction, UGS isolation, kidney capsule transplantation and analysis of xenografted urogenital tissues. **(B)** Gross images of representative xenografts from UGS tissue isolated from *R26*$^{mTmG/+}$*: Hes1Cre*$^{ERT2/+}$ (B1) or *R26*$^{mTmG/+}$*: Ar*$^{L/Y}$*: Hes1Cre*$^{ERT2/+}$ (B2) mice. **(C)** Graphical representation of xenograft weight from different genotype mouse grafts as labeled above. Please also see Supplemental Table 4 in the Supplemental data file. **(D)** and **(E)** Representative H&E staining of tissue sections from xenografts of *R26*$^{mTmG/+}$*: Hes1Cre*$^{ERT2/+}$ or *R26*$^{mTmG/+}$*: Ar*$^{L/Y}$*: Hes1Cre*$^{ERT2/+}$ mice. Blue arrows indicate flattened epithelial cells. **(F)** Co-IF analyses of graft tissues of *R26*$^{mTmG/+}$*: Hes1Cre*$^{ERT2/+}$ with GFP and different antibodies, AR (F1), E-cadherin (F2), CK8 (F3) or CK5 (F4) in xenografts. **(G)** Similar Co-IF analyses with graft tissues of *R26*$^{mTmG/+}$*: Ar*$^{L/Y}$*: Hes1Cre*$^{ERT2/+}$ as described in (F). White arrows indicate AR-deleted flattened cells. **(H)** Quantification of AR and GFP co-expressing cells in xenografts from different genotype mouse tissues as indicated above. Please see Supplemental Table 5

in the Supplemental data file. **(I)** Quantification of PCNA and GFP co-expressing cells in xenografts from different genotype mouse tissues as indicated above. Please see Supplemental Table 6 in the Supplemental data file. Scale bars: 2mm (4B1–2); 50μm, or 10μm in magnified views (4D-E); 100 μm, or 25 μm in magnified views (4F-G). Results are mean +/− SD of at least three independent samples per group. *: $P<0.05$.

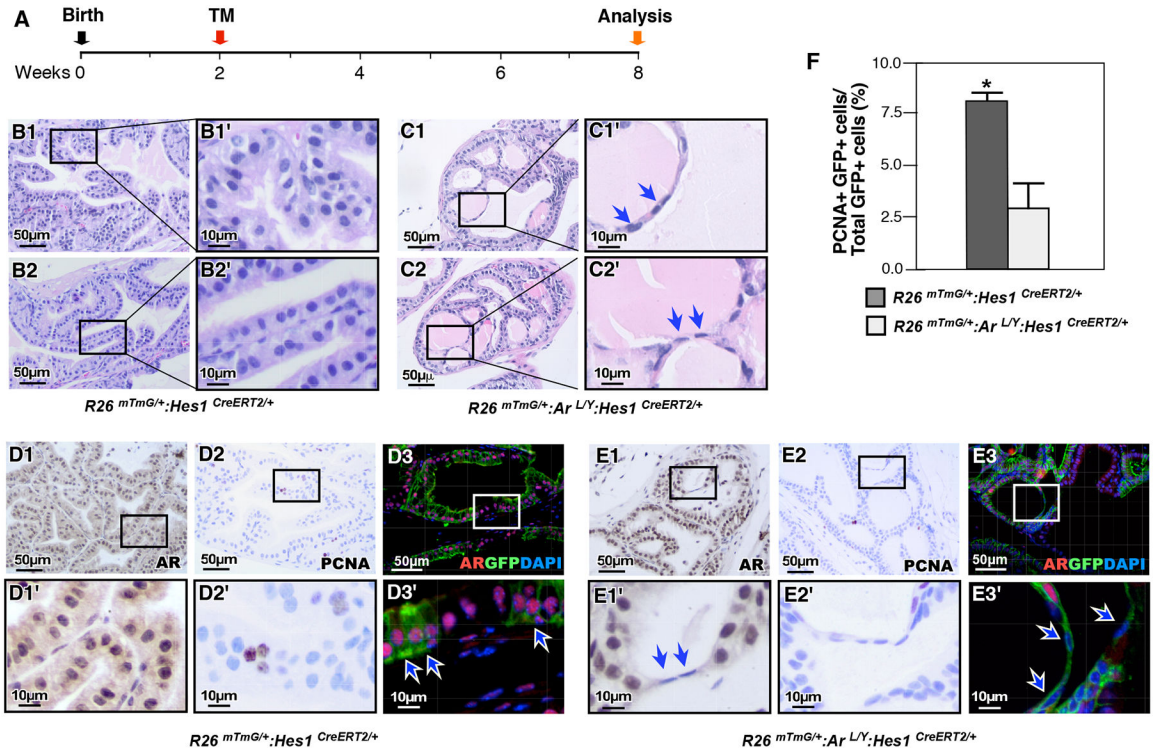


**Figure 5. Deletion of AR expression in prepubescent Hes1-expressing cells impairs prostate growth.**

**(A)** Schematic of experimental timeline for tamoxifen induction and analysis of prostatic tissues. **(B-C)** Representative H&E staining of prostate tissue sections from different genotypes mice as indicated above. Blue arrows indicate atrophic flattened epithelial cells resulting from loss of AR expression. **(D)** Immunohistochemical (IHC) and IF analyses of prostate tissues isolated from $R26^{mTmG/+}$: $Hes1Cre^{ERT2/+}$ mice using antibodies indicated above, AR (D1), PCNA (D2), or AR and GFP (D3). White arrows indicate AR and GFP co-expressing cells. **(E)** Similar analyses of prostate tissues isolated from $R26^{mTmG/+}$: $Ar^{L/Y}$: $Hes1Cre^{ERT2/+}$ mice were performed as indicated in D section. Arrows indicate AR-deleted flattened cells. **(F)** Quantification of PCNA and GFP co-expressing cells in prostate tissue sections from each genotype. Please also see Supplemental Table 7 in the Supplemental data file. Scale bars: 50 μm, or 10 μm in magnified views. Results are mean +/− SD of at least three independent samples per group. *: P <0.05.

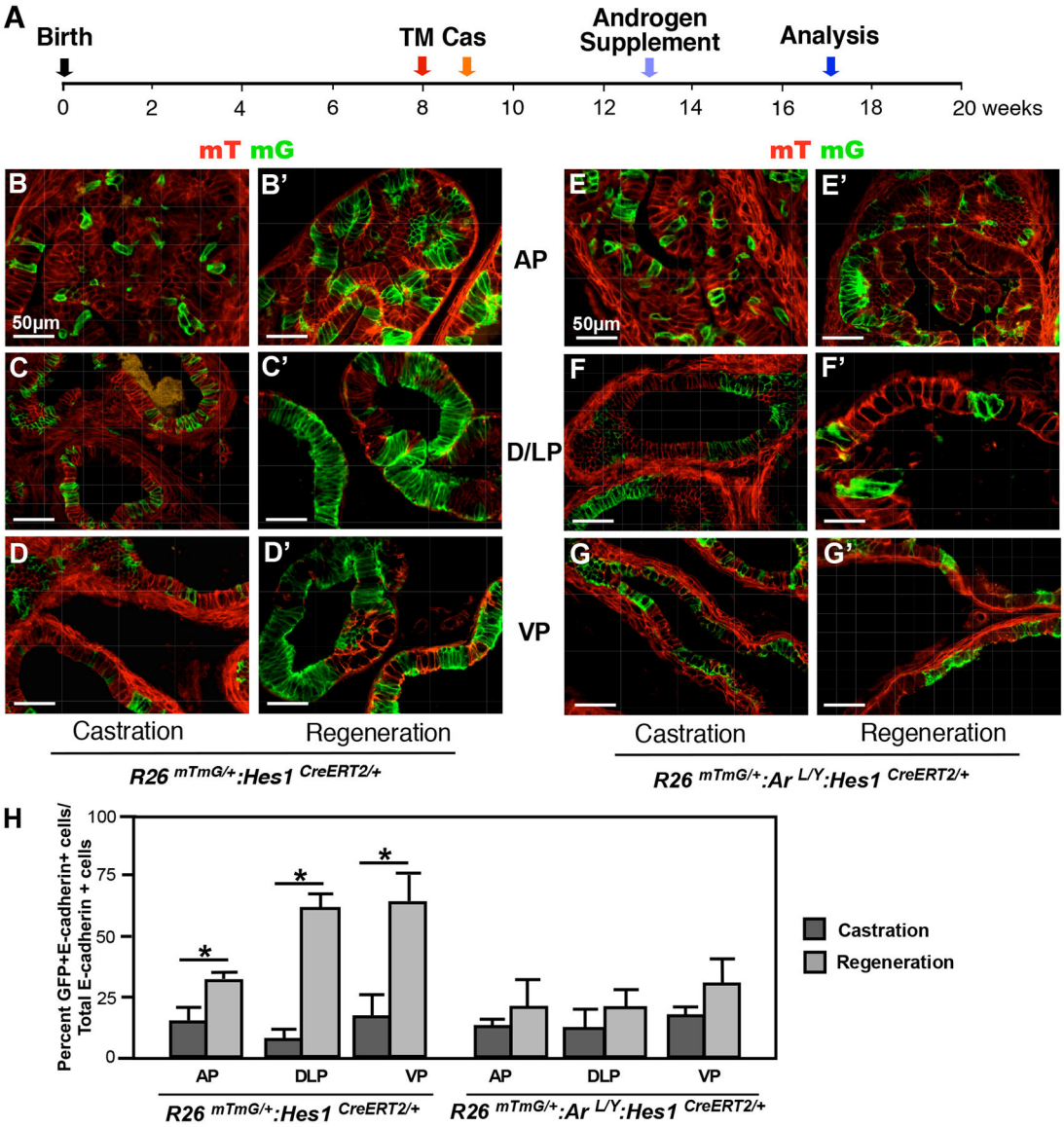


**Figure 6. Deletion of AR expression in Hes1-expressing cells impairs prostate regeneration.**

**(A)** Schematic of experimental timeline including tamoxifen induction, castration, regeneration and analysis of prostate tissues. Cas: castration. **(B-D)** mTmG analysis of different prostatic lobes in *R26*$^{mTmG/+}$*: Hes1Cre*$^{ERT2/+}$ mouse tissues prior to or post castration as labeled above. AP: anterior prostate, DLP: dorsolateral prostate, VP: ventral prostate. **(E-G)** Similar analyses were conducted in different prostatic lobes of *R26*$^{mTmG/+}$*: Ar*$^{L/Y}$*: Hes1Cre*$^{ERT2/+}$ mice. **(H)** Quantification of GFP and E-cadherin co-expressing cells in prostate lobes isolated from the indicated mice. Please also see Supplemental Table 8 in the Supplemental data file. Scale bars: 50 µm. Results are mean +/− SD of at least three independent samples per group. *P<0.05.